Electronic Supplementary Material (ESI) for Journal of Materials Chemistry A.

Supplementary information

Limitation of Ni-rich layered cathode in all-solid-state lithium batteries

Tae-Yeon Yu,[a] Han-Uk Lee,[a] Jin Wook Lee,[a] Sung-Min Park,[a] In-Su Lee,[a] Hun-Gi Jung,[b] and Yang-Kook Sun*[,a,c]

[a] Department of Energy Engineering, Hanyang University, Seoul 04763, Republic of Korea

[b] Center for Energy Storage Research, Korea Institute of Science and Technology (KIST), Seoul 02792, Republic of Korea

[c] Department of Battery Engineering, Hanyang University, Seoul 04763, Republic of Korea

*Corresponding author: yksun@hanyang.ac.kr

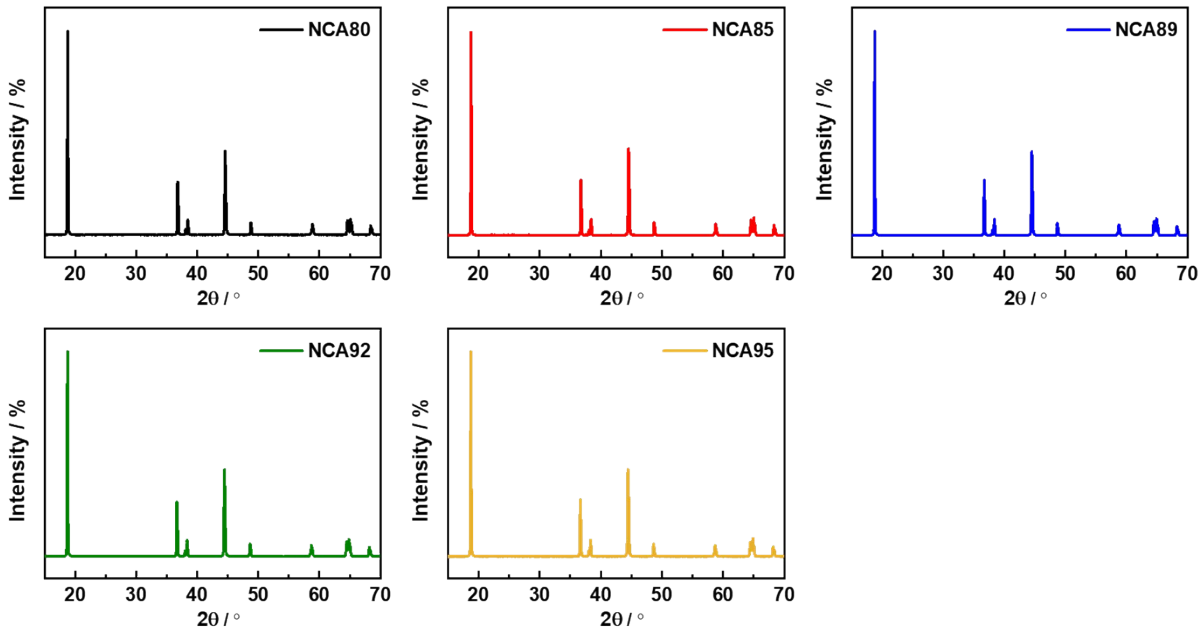

Fig. S1 XRD patterns of the NCA80, NCA85, NCA89, NCA92, and NCA95 cathodes.

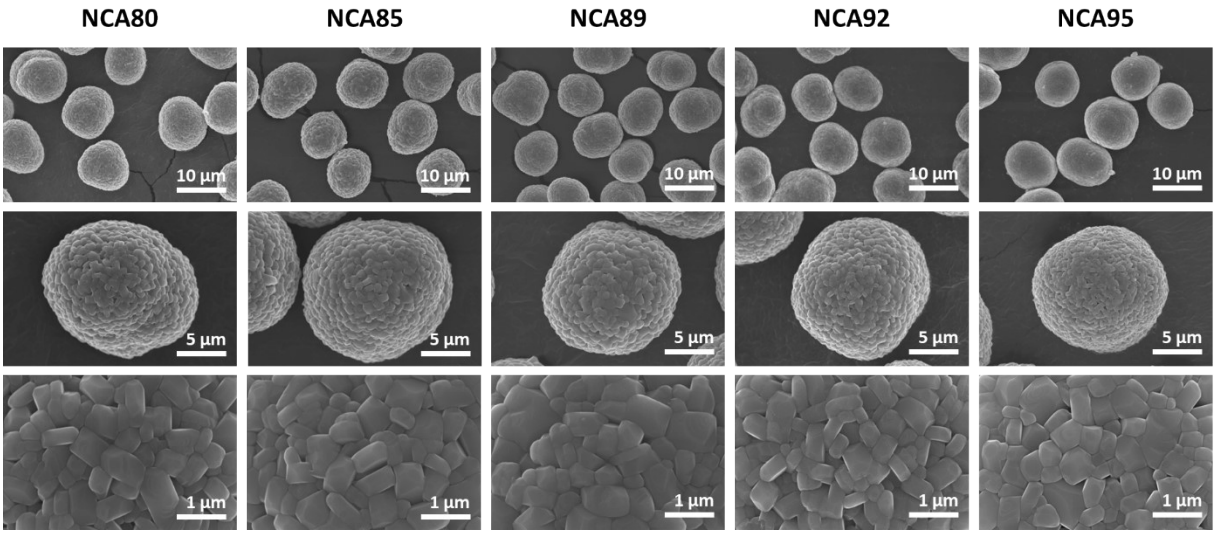

Fig. S2 Powder SEM images of the NCA80, NCA85, NCA89, NCA92, and NCA95 cathodes.

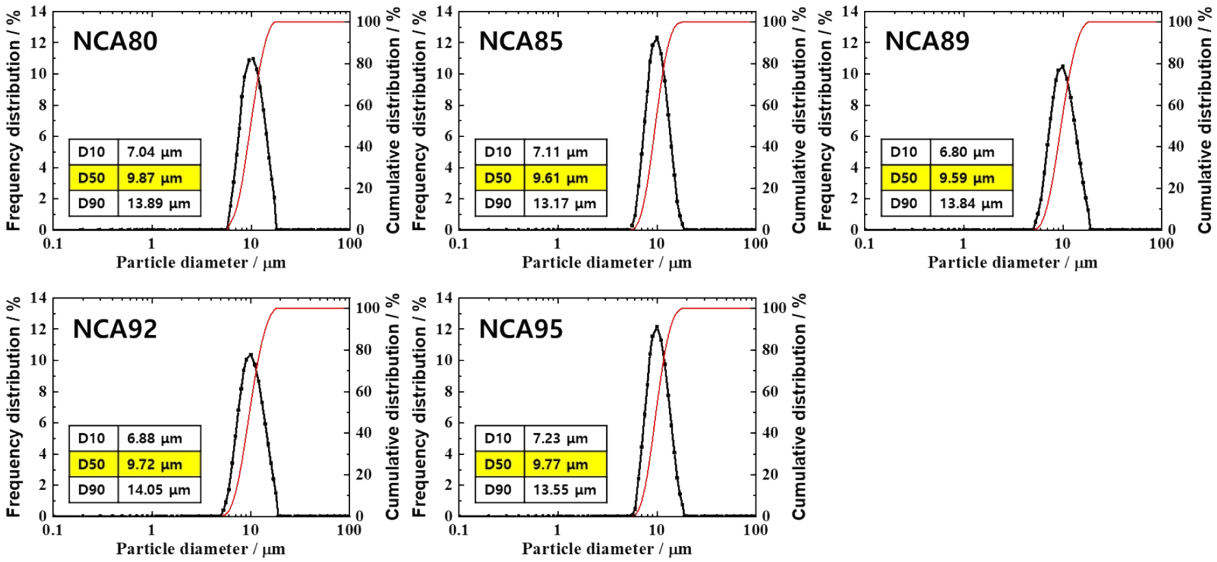

Fig. S3 Particle size analysis of the NCA80, NCA85, NCA89, NCA92, and NCA95 cathodes.

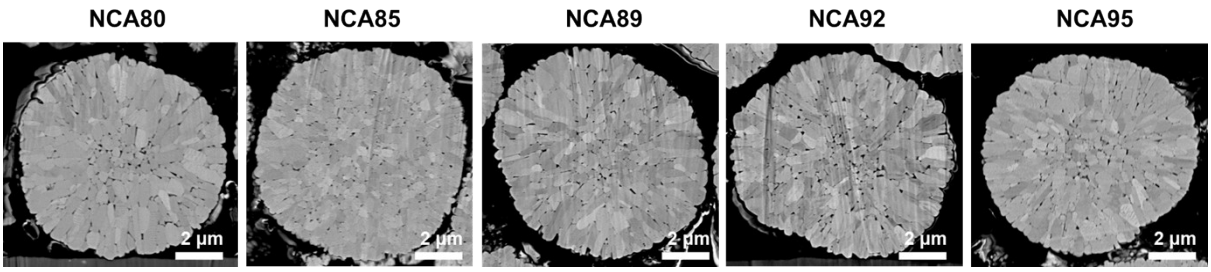

Fig. S4 Cross-sectional SEM images of as-synthesized NCA80, NCA85, NCA89, NCA92, and NCA95 cathodes.

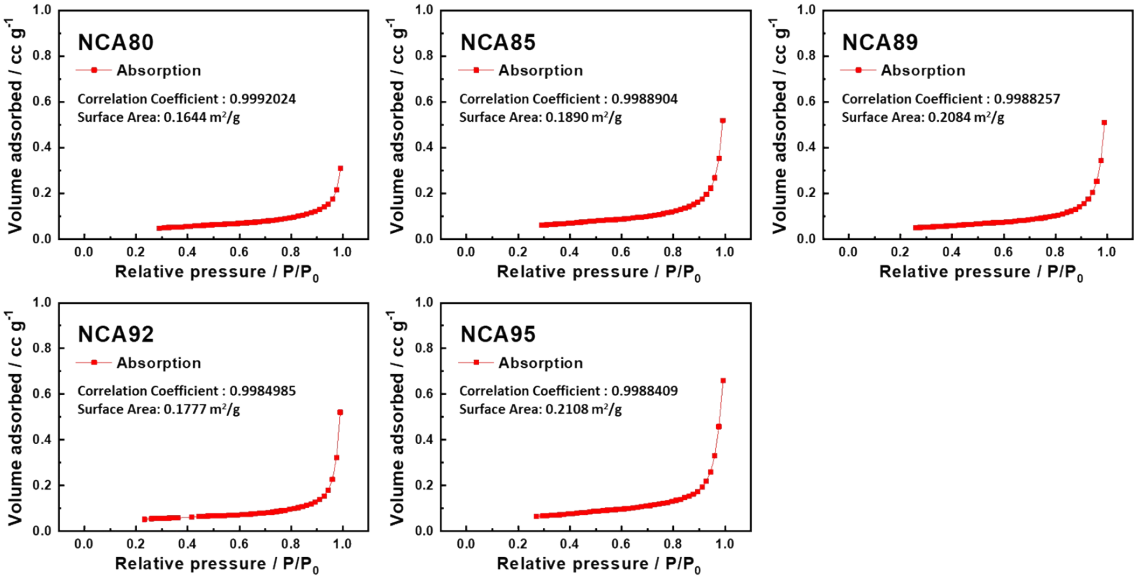

Fig. S5 The specific surface areas of the NCA80, NCA85, NCA89, NCA92, and NCA95 cathodes, as determined by BET analysis.

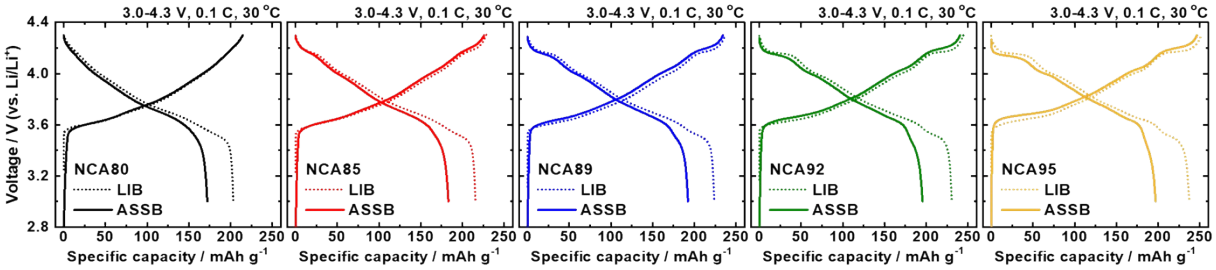

Fig. S6 The initial charge-discharge profiles of the NCA cathodes in LIB and ASSB at a current density of 0.1 C between 3.0-4.3 V.

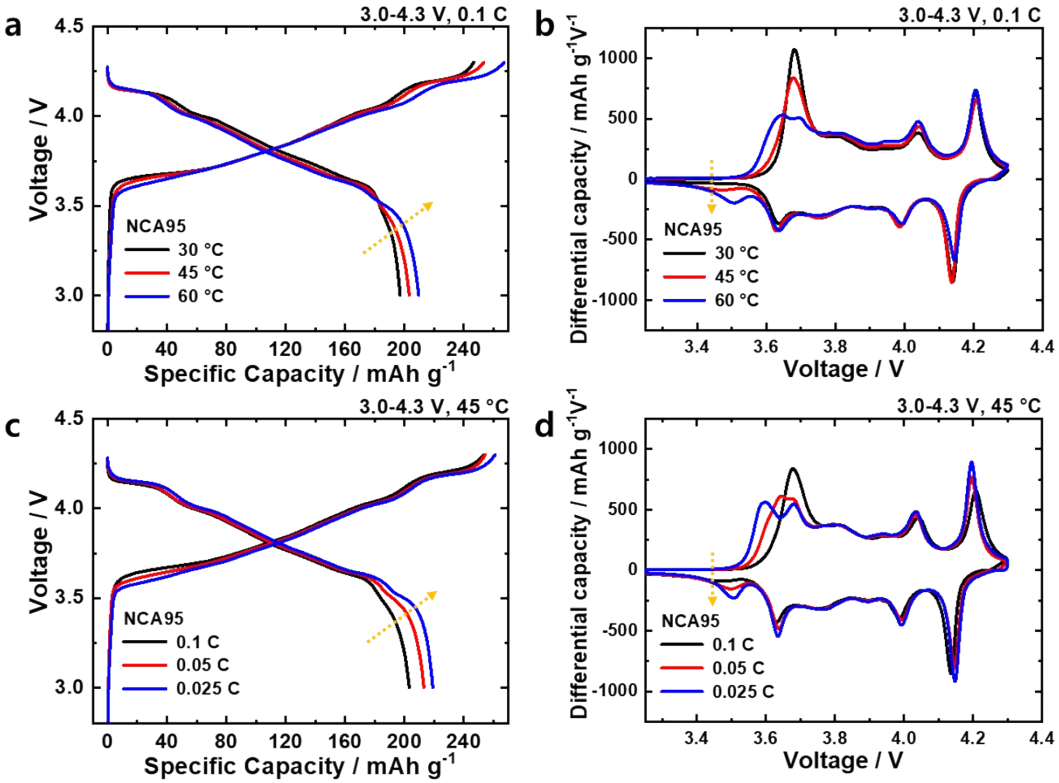

Fig. S7 The initial charge-discharge profiles and corresponding differential capacity (dQ dV^{-1}) curves of the NCA95 cathode measured (a,b) at various temperature with a current density of 0.1 C and (c,d) with various current densities at 45 °C between 3.0-4.3 V.

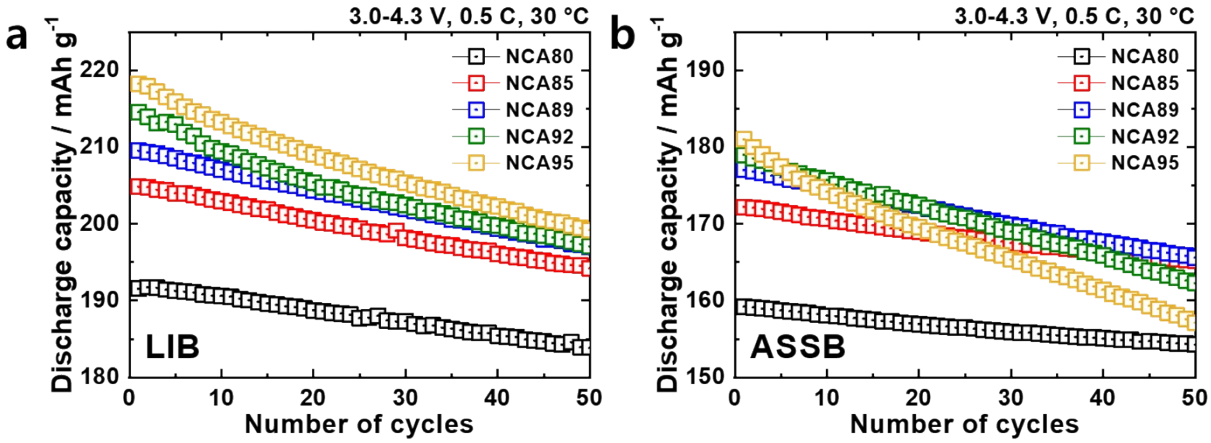

Fig. S8 Cycling performance of the NCA cathodes in (a) LIB and (b) ASSB

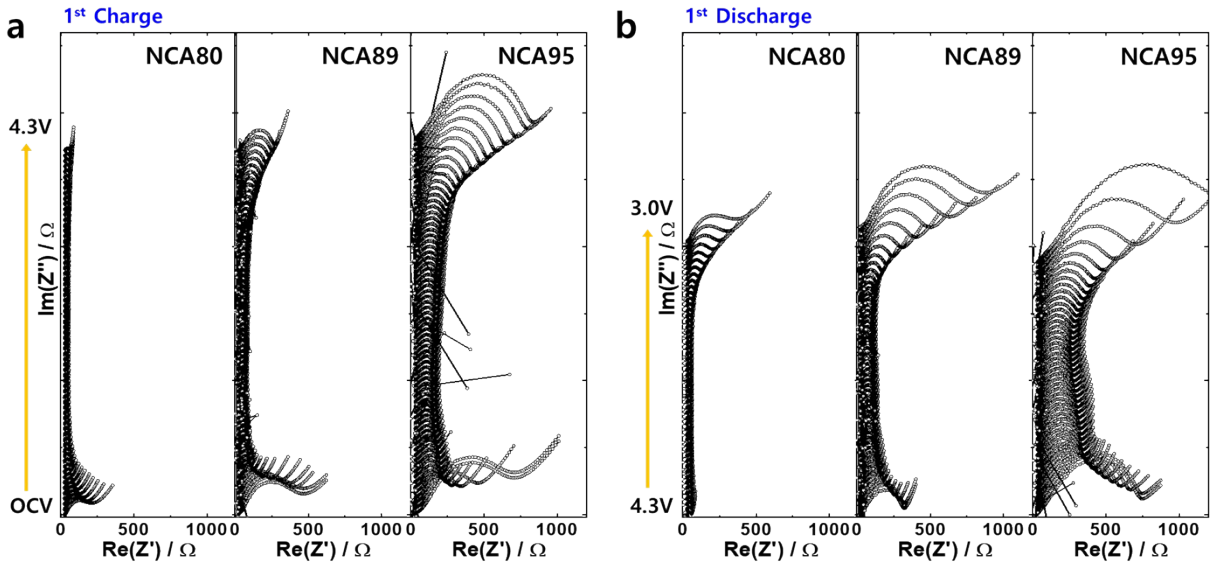

Fig. S9 Nyquist plots of the NCA80, NCA89, and NCA95 cathodes in ASSB during the initial charge/discharge process.

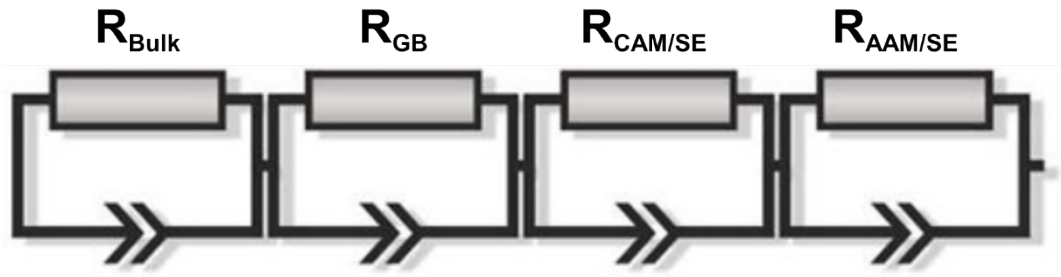

Fig. S10 An equivalent circuit is used to fit the experimental data.

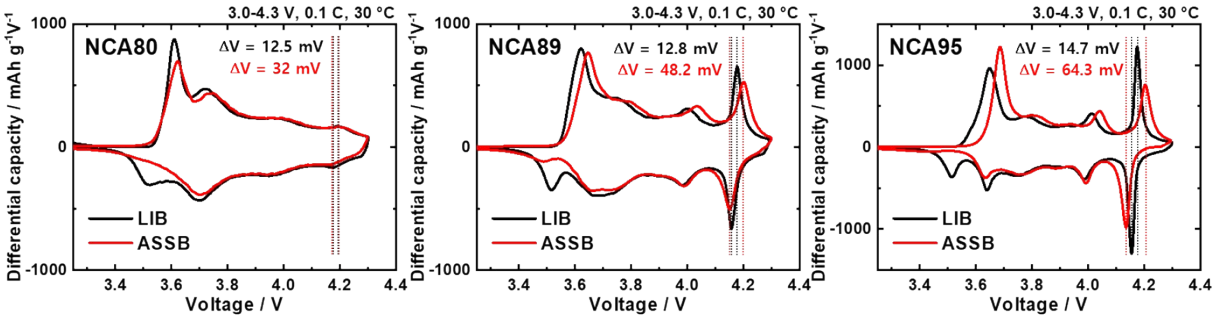

Fig. S11 Differential capacity (dQ dV^{-1}) curves of the NCA80, NCA89, and NCA95 cathodes for comparison between LIB and ASSB.

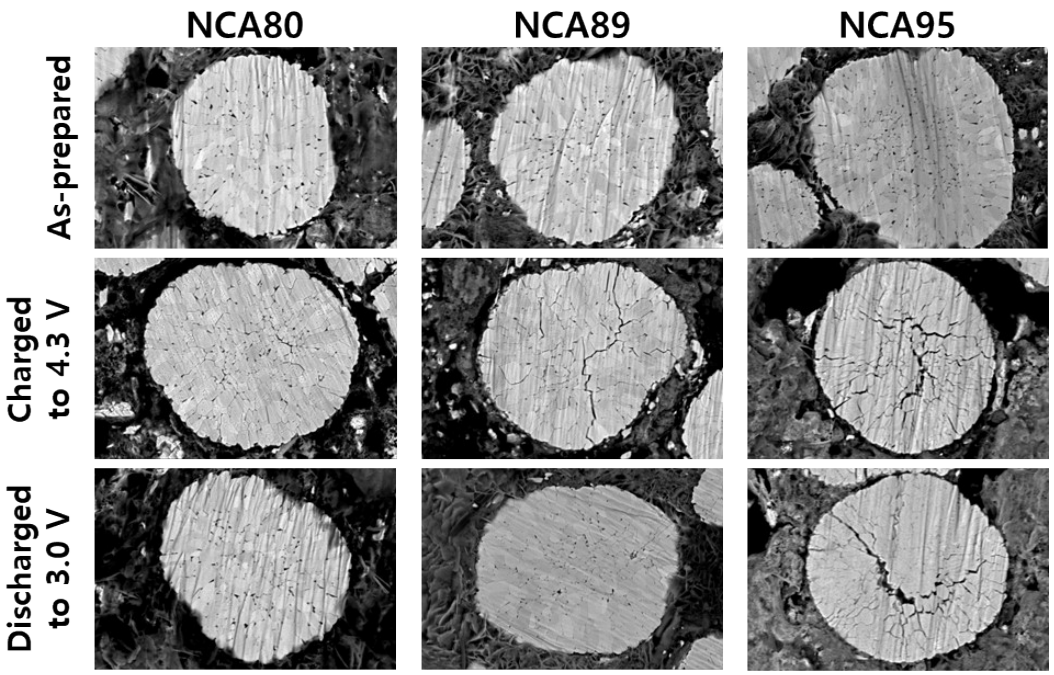

Fig. S12 Cross-sectional SEM images of the NCA80, NCA89, and NCA95 cathodes before and during the initial cycle.

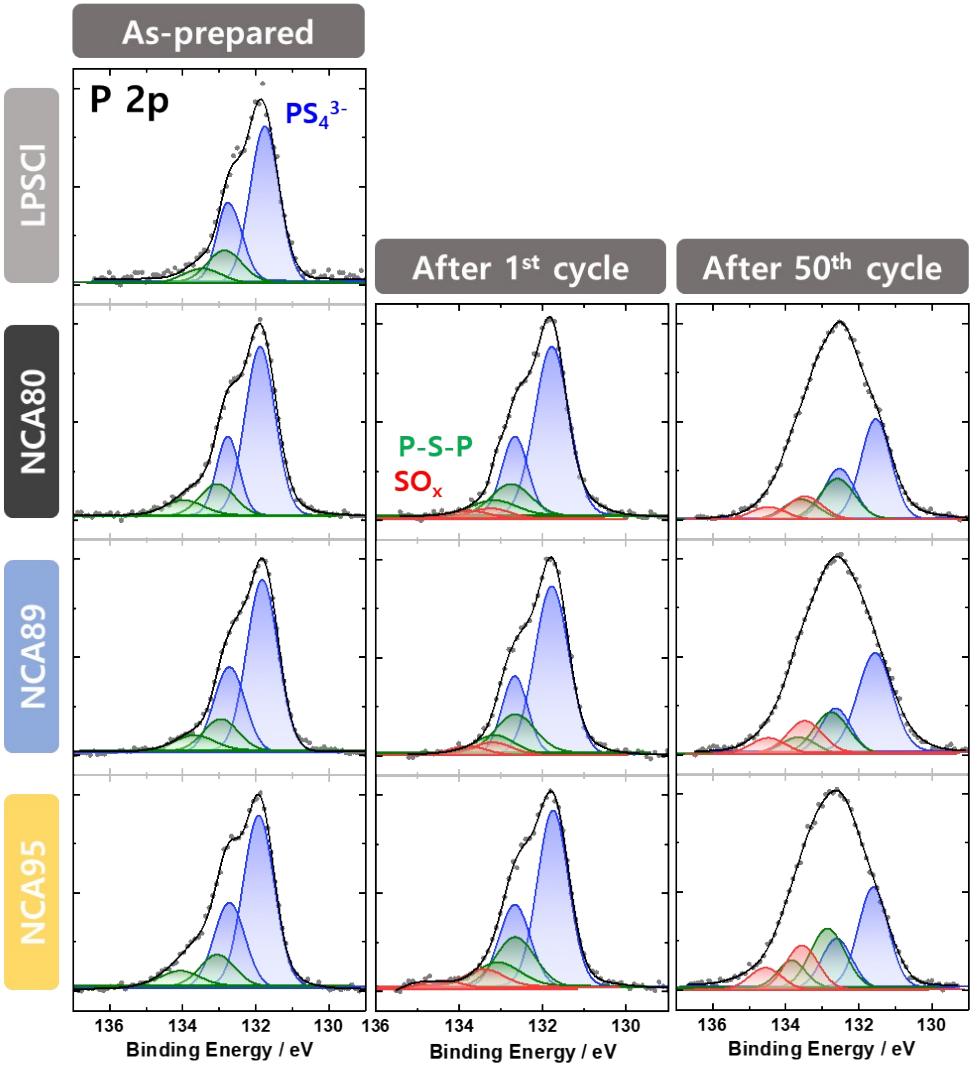

Fig. S13 Ex-situ P 2p XPS spectra of the pristine LPSCl solid electrolyte and cathodes before cycling, after the initial cyclem and after 50 cycles.

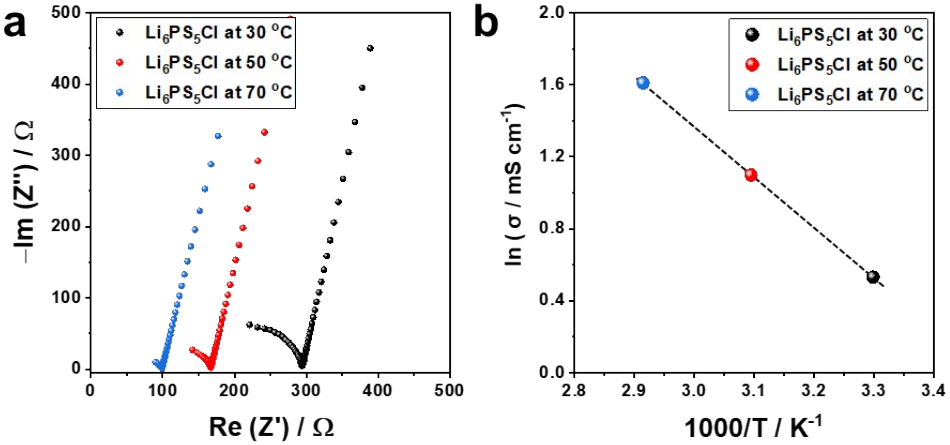

Fig. S14 (a) Nyquist plots and (b) Arrhenius plots of LPSCl powders at a temperature range of 30-70 °C.

Table S1. ICP-OES results of the as-prepared cathode materials

	Metal stoichiometry determined by ICP-OES (at. %)			
Sample	Target composition	Ni	Co	Al
NCA80	$[Ni_{0.80}Co_{0.17}Al_{0.03}]O_2$	80.62	17.03	2.35
NCA85	$[Ni_{0.85}Co_{0.13}Al_{0.02}]O_2$	84.99	13.47	1.54
NCA89	$[Ni_{0.89}Co_{0.10}Al_{0.01}]O_2$	89.17	10.03	0.80
NCA92	$[Ni_{0.92}Co_{0.07}Al_{0.01}]O_2$	92.05	7.14	0.81
NCA95	$[Ni_{0.95}Co_{0.04}Al_{0.01}]O_2$	95.37	3.80	0.83

Table S2. Results of the refinement of the XRD data.

Lattice parameters				
Sample	*a*-axis [Å]	*c*-axis [Å]	Volume [Å^3]	Cation mixing [%]
NCA80	2.8624	14.1755	100.587	0.3
NCA85	2.8667	14.1825	100.938	0.4
NCA89	2.8689	14.1851	101.110	0.7
NCA92	2.8708	14.1903	101.282	0.8
NCA95	2.8719	14.1956	101.395	1.2